THE APPROACH OF CHAOS IN DEFORMED NUCLEI

J. Carbonell, F. Brut, R. Arvieu, J. Touchard

JOURNAL DE PHYSIQUE
Colloque C6, supplément au n°6, Tome 45, juin 1984

THE APPROACH OF CHAOS IN DEFORMED NUCLEI

J. Carbonell, F. Brut, R. Arvieu and J. Touchard*

Institut des Sciences Nucléaires, 53, Avenue des Martyrs, 38026 Grenoble Cedex, France
**Institut de Physique Nucléaire, Division de Physique Théorique, B.P. n° 1, 91406 Orsay, France*

Résumé - On décrit l'organisation de l'espace de phase pour un neutron dans un potentiel déformé (A=16). La région où l'on trouve les trajectoires chaotiques est précisée. On construit numériquement la surface énergie-action pour la topologie la plus simple. On calcule enfin des énergies semi-classiques.

Abstract - The phase space of the trajectories of one neutron in a deformed single particle potential is sketched for A = 16. The region of occurrence of the chaotic trajectories is found. The energy action-surface is plotted for the simplest topology. Semi-classical energies are derived.

I - INTRODUCTION

The semiclassical method of quantization W.K.B. or E.B.K. is well adapted to the systems which are integrable in classical mechanics, i.e. which possess as many integrals of motion in involution as independent degrees of freedom. For those systems the trajectories are essentially divided into two classes : the periodic orbits and the quasi-periodic ones. It is well known that if the manifold defined by the intersection of the constants of motion is compact and connex that the trajectories lie on tori /1/ in phase space. The classical action-angle variables are adapted to this situation : the actions can then be interpreted as the radii of the tori. In an another communication to this workshop /2/ we have shown that the quantum mechanical spectrum of the single particle energies of one neutron in a spherical potential can be understood by studying the geometrical properties of the energy-action surface.

In this communication we want to discuss the problems which arise when a deformation of the potential is introduced . We have already briefly sketched /3/ the classical situation on which there has also been a thesis by one of us /4/. Our aim will be first to review a few results of ref. 4, and, secondly, to give an example, the simplest possible one, in which the energy action surface has been constructed and the semiclassical energies obtained.

When the Buck-Pilt potential also used in ref. 2 is given an ellipsoidal deformation by making the transformation

$$r = \sqrt{x^2 + y^2 + z^2} \longrightarrow \sqrt[3]{R_1 R_2^2}\ \sqrt{\frac{x^2 + y^2}{R_2^2} + \frac{z^2}{R_1^2}} \qquad (1)$$

(in the following we will use $\mu = R_1/R_2$; $\lambda = \sqrt[3]{R_1 R_2^2}/a$ the total angular momentum is not conserved and there is no new constant of motion in place of L. However L_z is conserved. If we consider the plane trajectories (with $L_z = 0$) of constant energies we need to explore numerically the phase space (3 dimensional) in order to examine the dimension of the manifold on which lie the trajectories.

The numerical and the theoretical works performed during the last twenty years on the theory of dynamical systems have led to a qualitative description of the phase space of quasi integrable systems. The work by Henon and Heiles /5/ is often quoted as one of the first numerical experiment on a simple but non integrable system for which this description was discovered. Let us briefly mention the known results.

Let ε be any parameter which characterizes the non linearity like the excitation energy, or the deformation or the size of the potential. There exists a critical value ε_c which allows to separate the topological flow into two parts :

a) for $\varepsilon < \varepsilon_c$ the system looks mostly like an integrable one : there exists periodic orbits and quasi-periodic orbits. The chaotic orbits exist only at a microscopic level. Because of the quasi-integrability and the dominance of the tori in phase space the EBK semiclassical method of quantization is possible there /6/. However there is a considerable complication of the phase space. Indeed every periodic orbit bifurcates and gives rise, for any infinitesimal change of ε, to new periodic orbits and to new tori. As we will see below there exists techniques which allow to locate the value of ε for which a given bifurcation occurs. The main problem, still unsolved to our knowledge, lies in the maximum size of the tori which surround a given periodic orbit and of the location of the separatix between the different families.

b) for $\varepsilon > \varepsilon_c$ the volume of the tori decreases rapidly with ε to the benefit of the chaotic orbits which tend to occupy the whole of phase space. In this region of parameters the phase space is even more complex than in the preceding one. So complex that it becomes hardly possible to find tori which fulfill the semiclassical conditions.

The critical value ε_c is often quoted as the threshold of macroscopic stochasticity. For $\varepsilon < \varepsilon_c$ it is rather difficult to find out chaotic orbits numerically.

The evolution just described has a so called "generic" character, i.e. it is qualitatively correct for most of the quasi-integrable systems whatever is the potential or the parameter ε.

In the following we want to sketch first how this behaviour is seen for the phase space of $L_z = 0$ trajectories in A = 16, i.e. $\lambda = 4.898$ and $1 < \mu < 2$. For the sake of space limitation we will not discuss other values of A nor the other values of L_z (which would correspond to non planar trajectories) see ref. 4.

II - THE PHASE SPACE OF DEFORMED ^{16}O

a) The first question is whether the deformed potential is integrable or not. If the non integrability prevails it is necessary to locate the threshold in terms of the excitation energy $\eta = 1 - \frac{E}{V_o}$ or of the deformation μ.

Fig. 1 presents an example of a chaotic trajectory. In the bottom of the figure the trajectory is plotted in the configuration space (ρ means x or y). The upper part represents the Poincaré section of the same trajectory, i.e. the set of the successive values of its interactions (ρ) and projections of momentum (p_ρ) on the y axis (with the restriction that $p_z > 0$). The set of points so obtained clearly do not form an invariant curve, the trajectory belongs to a manifold of higher dimension. The existence of chaotic trajectories is usually taken as a numerical indication that the potential is not integrable. The large values of the parameters : $\mu = 1.5$ and $\eta = 0.99$ (i.e. near the dissociation energy) indicate that it has been necessary to look for rather extreme conditions in order to observe a chaotic trajectory. In other words the values μ_c and η_c are rather large. In the case of A = 16 our numerical experiments conclude that the chaotic trajectories do not

appear in the domain

$$1 \lesssim \mu < 1.3 \qquad\qquad 0 \lesssim \eta < 0.9$$

The precise location of the threshold necessitates an extremely detailed study of the Poincaré plane such as Fig. 4 of Ref. 3 which shows that $\eta_C \simeq 0.95$ for $\mu = 1.5$ while Fig. 4 of the present paper shows that $\eta_C > 0.95$ for $\mu = 1.4$. In other words the chaotic region corresponding to the $L_z = 0$ trajectories of A = 16 is limited to a rather thin skin of values of η of width $\Delta\eta \simeq 0.05$ for $\mu > 1.3$.

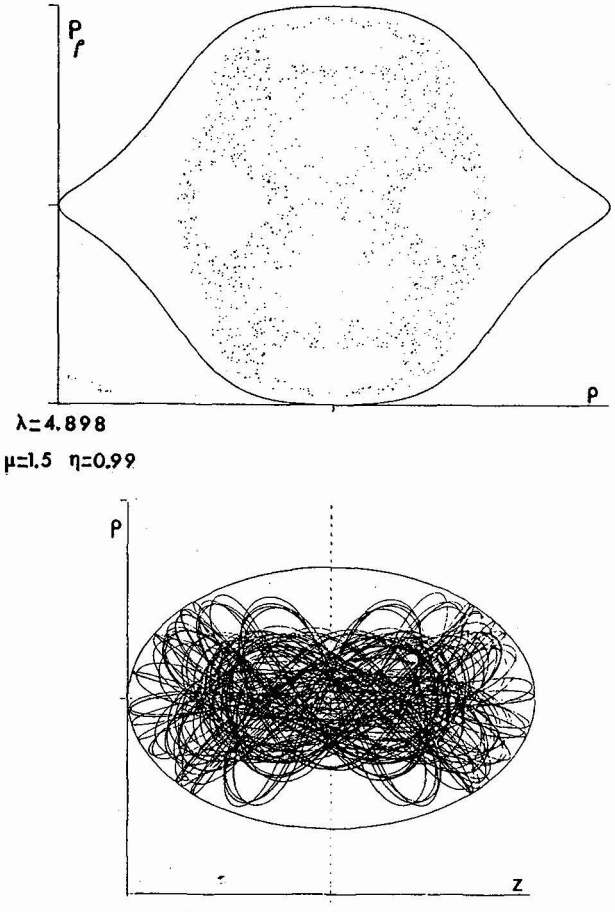

Fig. 1 - A chaotic trajectory of the deformed well for A = 16. The upper part is the Poincaré section of the trajectory represented in the lower part in configuration space.

b) The second question is to analyze in detail the structure of the phase space below the threshold of chaoticity. As we mentioned before there are infinitely many bifurcations of the periodic trajectories. It is out of question simply to enumerate the periodic trajectories which occur in a given Poincaré section. However in our potential two trajectories play a particular role : the linear trajectories along the ρ and z axis of symmetry of the potential. These trajectories are simple and easily found numerically and generate the most important bifurcations which one may call the bifurcations of first generation.

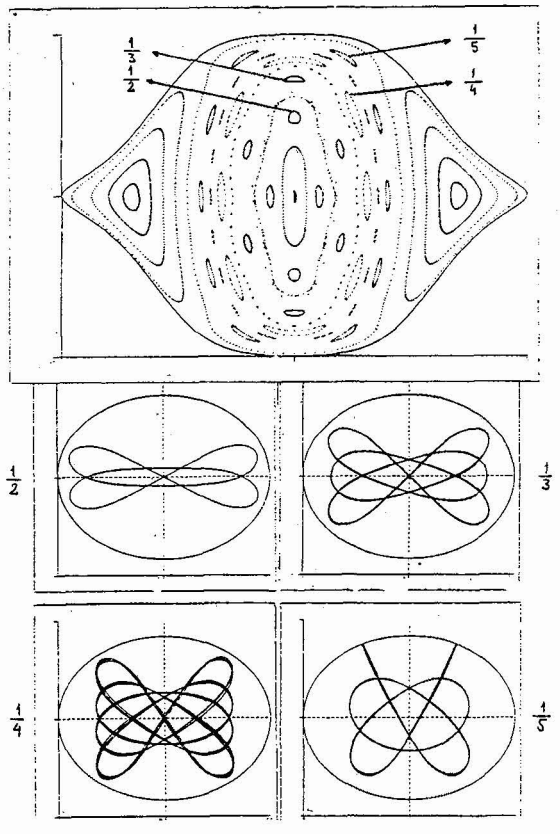

Fig. 2 - The upper part is the Poincaré section $\{\rho, p_\rho\}$ of the deformed well for $\mu = 1.2$, $\eta = 0.99$. The four lower figures represent Lissajous-like trajectories found at the place indicated above.

A numerical procedure has been developed in Ref. 4 which allows to study the properties of the mapping in the vicinity of the linear periodic trajectories. The trajectories which arise through the bifurcations of the linear trajectories are Lissajous-like figures. Some are represented on Fig. 2. These curves are surrounded by tori which form in the Poincaré plane islands of different sizes. Some of the islands (the majority !) are so tiny that they cannot be detected numerically, however a few islands can always be detected like in Fig. 2. The center of the islands is the place of the periodic trajectory. The value of the parameter where the Lissajous figure is degenerate with the linear trajectory marks the birth of this figure. It is found by the following method :

Let M_ρ be the non linear mapping in the $\{\rho, p_\rho\}$ Poincaré plane which makes the iteration between the k^{th} and the (k+1) th intersections : $M_\rho \begin{pmatrix} \rho \\ p_\rho \end{pmatrix}_k = \begin{pmatrix} \rho \\ p_\rho \end{pmatrix}_{k+1}$.

Let us consider this mapping near the origin which is a fixed point of the mapping. If ρ and p_ρ are very small M_ρ coincides with its linear part. It is known that if $|\mathrm{Tr}\, M_\rho| < 2$ the fixed point is elliptical while if $|\mathrm{Tr}\, M_\rho| > 2$ the fixed point is hyperbolic. A bifurcation occurs whenever $|\mathrm{Tr}\, M_\rho|$, or any of its power $|\mathrm{Tr}\, M_\rho^{\,n}|$, equal 2. (It can be proved / 4/ that in our potential $\mathrm{Tr}\, M_\rho \geq -2$, therefore the singular value is +2). If $\mathrm{Tr}\, M_\rho$ is written as $2 \cos \alpha$, for $|\mathrm{Tr}\, M_\rho| < 2$, the value of α is a continuous function of the parameters μ and η. It is then easy to find the points where $\alpha = 2\pi \frac{m}{n}$ for which $\mathrm{Tr}\, M_\rho^n = 2$. At each of these values a Lissajous'curve is created for $n > 1$.

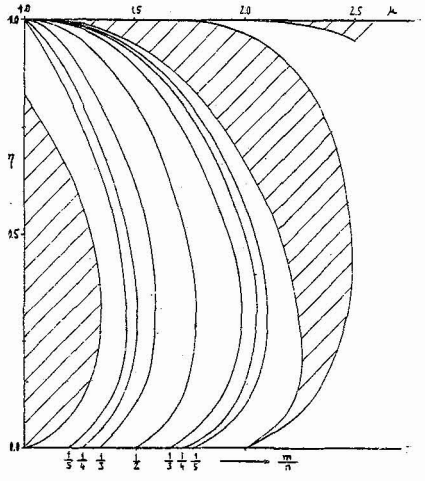

Fig. 3 – Each curve represents the values of η and μ where equation (2) is satisfied for values of $\frac{m}{n}$ indicated at the bottom. M_ρ is the mapping in the vicinity of the linear trajectory along the long (z) axis.

On Fig. 3 the points where

$$\mathrm{Tr}\ M_\rho(\mu,\eta) = 2 \cos 2\pi \frac{m}{n} \qquad (2)$$

are plotted with μ and η as coordinates axis for $\frac{m}{n} = \frac{1}{2}, \frac{1}{3}, \frac{1}{4}$ and $\frac{1}{5}$ as well as the curves with m = n. The latter curves define regions in which Tr $M_\rho > 2$ where no bifurcations are possible. The Poincaré section shown in Fig. 2 illustrates this situation. Periodic trajectories corresponding respectively to $\frac{m}{n} = \frac{1}{2}, \frac{1}{3}, \frac{1}{4}, \frac{1}{5}$ are met when going away from the center of the mapping for $\mu = 1.2$. The location of the corresponding bifurcations are made by order of decreasing energy on Fig. 3. The chaotic regions are not represented on Fig. 3 which has been obtained only by a local study of the mapping near $\rho = 0$.

In the region where the center of the mapping bifurcates the center is an elliptic point like for the harmonic oscillator. It turns out that in this region there is a very broad range of values of parameters for which the tori around the Lissajous curves are very small. It is possible to say that in this region the topology is that of the harmonic oscillator. An example is given with Fig. 4 where no other torus is seen for $\eta < 0.85$ but those defined by the invariant curves which look like ovals surrounding the center.

In Fig. 4 the tori issued from bifurcations of first generation are seen only for $\eta = 0.90$. If $\eta < 0.85$ the picture of the Poincaré map resembles much the left upper side of Fig. 4.

Fig. 3 shows that this picture is valid locally, indeed two parts of phase space with a completely different topology are shown as the dashed area issued from $\mu = 2$ and the other one around $\mu = 1$.

A preliminary conclusion is that for $1.3 < \mu < 2$ there is a region where the topology of the harmonic oscillator is dominant and therefore the motion can be quantized with the rules used for the harmonic oscillator.

Fig. 5 shows an example where two topologies arise. There $\mu = 1.06$, $\eta = 0.7$. The harmonic oscillator-like trajectories are seen as curves with hyperbolic-like caustics while the other curves have elliptic-like caustics. We have not yet performed the quantization of the cases where two or several topologies are present at the same time.

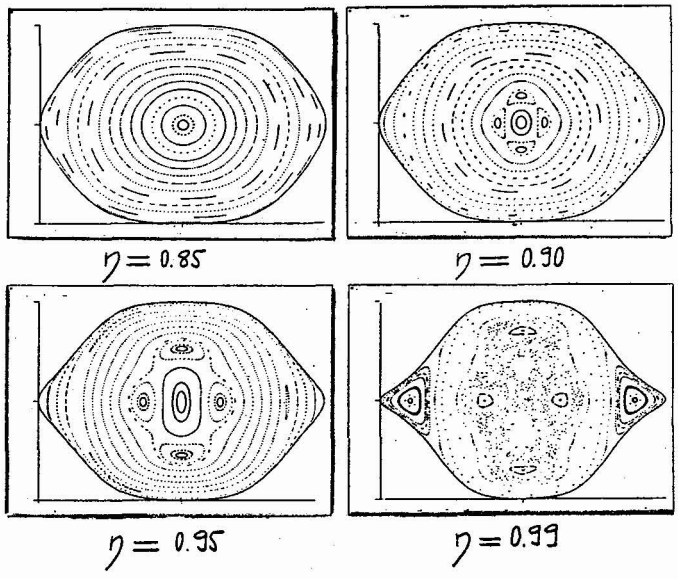

Fig. 4 - Poincaré sectiond for $\mu = 1.4$ at several energies.

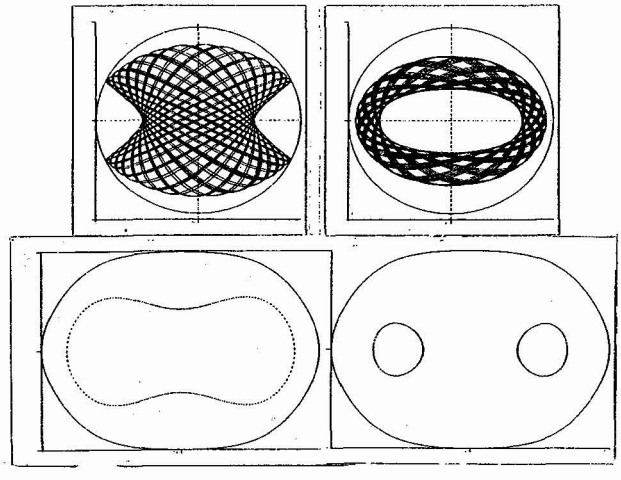

Fig. 5 - Two trajectories with different topologies in configuration space (upper part) and their Poincaré section (lower part). Here $\mu = 1.06$ and $\eta = 0.7$ for both trajectories.

III - QUANTIZATION IN THE CASE OF THE SIMPLEST TOPOLOGY

If the majority of the orbits of the deformed potential are similar to those of Fig. 4 for $\eta = 0.80$, they can be quantized with the same rules as the harmonic oscillator. Let p_ρ and p_z be the projections of the momentum of the particle on the ρ and z axis while it intersects the ρ and z axis respectively and let C_ρ and C_z be the set of values of ρ and z taken during these intersections, the actions are defined as

$$I_z = \oint_{C_z} p_z \, dz = (n_z + \tfrac{1}{2})\hbar \qquad (3)$$

$$I_\rho = \oint_{C_\rho} p_\rho \, d\rho = (n_\rho + 1)\hbar \qquad (4)$$

Using K.A.M. theorem, "most of the trajectories lie on tori", and since the topology (at least the "macroscopic ones" !) is that of the harmonic oscillator we are able to define a surface energy action :

$$E = E(I_z, I_\rho) \qquad (5)$$

for all the trajectories with this topology. The semiclassical energies are those values of E for which eq.(3) and (4) are satisfied. Fig. 6 shows trajectories belonging to five set of energies : η = 0.4; 0.6; 0.7; 0.8. The set of points with equal energies are almost aligned on parallel straight lines.

However the surface does not exist for every value of I_ρ and I_z! Indeed there are two important differences with the integrable case :

a - It is not continuous but it contains infinite set of tiny holes (the destroyed tori) : the surface is porous;

b - For large η (as seen on Fig. 4 for η = 0.95 and 0.99 the surface is destroyed.

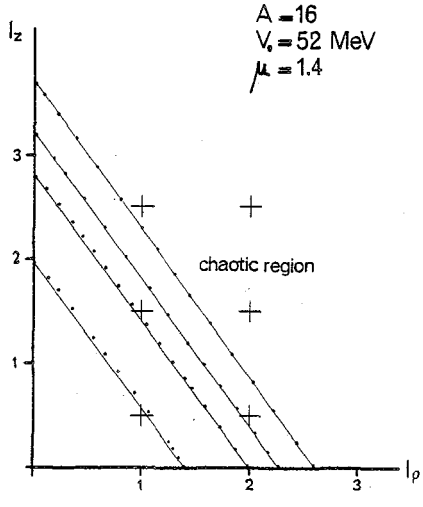

Fig. 6 - Section of the energy action surface in the non integrable case with μ = 1.4. The points indicate the tori for which the actions have been calculated. The tori cannot be easily or simply cannot be found for η > 0.8. The crosses locate the position of tori which fulfill the semiclassical conditions Eq. 3 and 4.

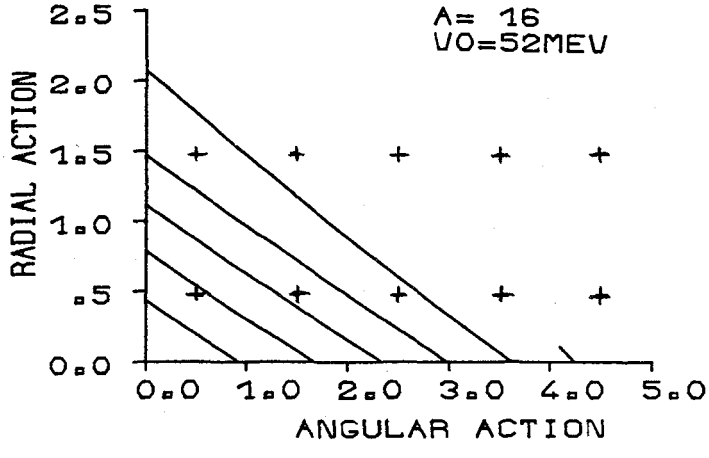

Fig. 7 - Same as Fig.6 for the integrable case μ = 1.

Fig. 6 illustrates in a very remarkable way the power of the K.A.M. theorem. It can be compared to Fig. 7 which represents the energy action surface $E(I_r,\ell)$ of ^{16}O for $\mu = 1$. Both Fig. 6 and 7 share the same property and give the same message : except near $\eta \sim 0.90$ the energy action surface is planar and the spectrum is harmonic. This property is conserved even in the non integrable situation ! However near $\eta \sim 0.90$ the surface is non planar for $\mu = 1$ this means that there are nonlinearity in the motion. For $\mu = 1.4$ this nonlinearity produces a destruction of the energy action surface and the impossibility of using properly the EBK method.

The comparison of the semiclassical and quantum eigenvalues of $\mu = 1$ and 1.4 is made in Table 1. This table shows that there is no essential difference between the two cases except in the chaotic region.

IV - CONCLUSION

In conclusion it seems that below the threshold of stochasticity it is possible to use properly the semiclassical EBK method of quantization and that this method is able to explain the properties of the spectrum with the same quality as for the integrable case. However in order to realize wholly this program we need to face the changes of topologies like those of Fig. 5.

	spherical $\mu = 1$ (integrable)		deformed (L_z=0) $\mu = 1.4$ (not integrable)	
	E_Q	$E_Q - E_{sc}$	E_Q	$E_Q - E_{sc}$
1s	-32.588	-0.119	-32.324	+ 0.260
1p	-18.024	-0.776	-20.718	- 0.364
2s	- 4.426	-0.789	- 8.901	- 0.832
1d	- 3.791	-1.2675	- 1.615	chaos

Table 1

REFERENCES

/1/ ARNOLD V.I., Méthodes Mathématiques de la Mécanique Classique, Editions MIR - Moscou (1967)

/2/ CARBONELL J., BRUT F., TOUCHARD J. and ARVIEU R., communication to this workshop

/3/ CARBONELL J. and ARVIEU R., Nuclear fluid dynamics, (1983) Trieste 141

/4/ CARBONELL J. thèse de 3ème Cycle - Université de Grenoble (1983) ISN 83-07

/5/ HENON M. and HEILES C., Astron. Journal 69 (1964) 73

/6/ PERCIVAL I., Advances in Chem. Phys. 36 (1977) 1